Red antenna states of photosystem I from Synechococcus sp. PCC 7002

ARTICLE *in* PHOTOSYNTHESIS RESEARCH · MARCH 2008

Impact Factor: 3.5 · DOI: 10.1007/s11120-007-9241-6 · Source: PubMed

Photosynth Res
DOI 10.1007/s11120-007-9241-6

REGULAR PAPER

Red antenna states of photosystem I from *Synechococcus* sp. PCC 7002

Marc Brecht · Jana B. Nieder · Hauke Studier · Eberhard Schlodder · Robert Bittl

Received: 6 September 2007 / Accepted: 6 September 2007

Abstract Absorption, fluorescence and single-molecule spectroscopy at low temperatures were used to elucidate spectral properties, heterogeneities and dynamics of the red-shifted chlorophyll a (Chla) molecules responsible for the fluorescence in photosystem I (PSI) from the cyanobacterium *Synechoccocus* sp. PCC 7002. The 77 K absorption spectrum indicates the presence of 2–3 red-shifted Chla's absorbing at about 708 nm. The fluorescence emission spectrum is dominated by a broad band at 714 nm. The emission spectra of single PSI complexes show zero-phonon lines (ZPLs) as well as a broad intensity distribution without ZPLs. The spectral region below 710 nm often shows ZPLs, they form a spectral band with a maximum at 698 nm (F698). The region above 710 nm is dominated by broad intensity distributions and the observation of ZPLs is less frequent. The broad distributions are due to the emission of the C708 Chla's and the emission from F698 stems from a Chla species absorbing at the blue side of P700. The properties of these two emissions show a close relation to those of the C708 and C719 pools observed in *T. elongatus*. Therefore an assignment of F698 and C708 to Chla-species with similarities to C708 and C719 in *T. elongatus* is proposed.

M. Brecht · J. B. Nieder · H. Studier · R. Bittl (✉)
Fachbereich Physik, Freie Universität Berlin, Arnimalle 14, 14195 Berlin, Germany
e-mail: Robert.Bittl@Physik.FU-Berlin.DE

E. Schlodder
Max-Volmer Laboratorium für Biophysikalische Chemie, Technische Universität Berlin, Strasse des 17. Juni 135, 10623 Berlin, Germany

Keywords Photosystem I · Single-molecule spectroscopy · *Synechoccocus* sp. PCC 7002 · Protein-cofactor interaction · Spectral diffusion · Energy landscape

Abbreviation

PSI	Photosystem I
Chla	Chlorophyll a
SMS	Single-molecule spectroscopy,
ZPL	Zero-phonon line
PW	Phonon wing
td	time-dependent

Introduction

The absorption spectra of PSI from green plants, algae, and cyanobacteria show the existence of Chla molecules absorbing at longer wavelength than P700, the primary electron donor of the reaction center, i.e., the lowest excited state of the antenna system lies below that of P700 (Brettel 1997). These red-shifted Chla molecules are often called the "red pool" or the long-wavelength chlorophylls (for a reviews, see (Gobets and van Grondelle 2001; Karapetyan et al. 2007)). Due to their spectral properties, Chla-multimers have been discussed as candidates for the red pool Chla (see e.g., Melkozernov et al. 2000; Schlodder et al. 2007). If the excitation energy is localized within these red pool Chla, the stored energy is no longer sufficient to directly excite P700 to P700*. Additional activation energy, e.g., thermal energy of the phonon bath, is necessary to excite P700 and start the charge separation process. The number and spectral position of red Chla differs remarkably between the PSI complex from different

organisms. For PSI from the cyanobacterium *Synechococcus* PCC 7942 two Chla were found to be responsible for the red absorption (Andrizhiyevskaya et al. 2002), whereas for the PSI from *Thermosynechoccocus elongatus* (*T. elongatus*, previously *Synechoccocus elongatus*) 7–9 Chla per monomer were found (Palsson et al. 1998; Byrdin et al. 2000). PS I core complexes of all organisms consist of two large subunits, PsaA and PsaB, and at least eight smaller subunits. Comparing the organization of the Chla's in the 2.5 Å structure from *T. elongatus* (Jordan et al. 2001) with those observed in the 3.4 Å structure from pea (Amunts et al. 2007), it appears that the positions and orientations of most Chla's in the PS I core are conserved between cyanobacteria and higher plants. Therefore the question concerning the assignment of the red states to molecules, the origin of the red-shift, and the physiological role of the red pool in different species remains puzzling (Sener et al. 2002; Gobets et al. 2003).

The well-resolved structural model for the cyanobacterium *T. elongatus* from X-ray crystallography (Jordan et al. 2001; Krauss et al. 1996; Fromme et al. 2001) is used as a reference structure for PSI in general, and PSI from *T. elongatus* has been used to investigate key properties of all types of PSI. Based on the X-ray structure, four possible candidates of Chla assemblies were proposed as origin of the red emission (Fromme et al. 2001). However, structural data alone allows only an tentative assignment and spectroscopic investigations, including hole-burning spectroscopy (Zazubovich et al. 2002) and single-molecule spectroscopy (Jelezko et al. 2000), are needed for its confirmation. Single-molecule spectroscopy (SMS) (Tamarat et al. 2000) serves as a method where ensemble averaging can be completely avoided and thus can be used to unravel information buried in spectra of large ensembles. As a consequence, spectral features that are characteristic for single molecules become visible. At low temperature these are a narrow zero-phonon line (ZPL) and a broad phonon wing (PW). The ZPL belongs to an electronic transition without phonon creation or annihilation. The PW, in the emission spectra on the low energy side of the ZPL, is due to the interaction of the chromophore with its surrounding, leading to the excitation of phonons (lattice vibrational modes). Relative to the ZPL the maximum of the PW is shifted to the red by 20–30 cm^{-1} and has a width of $\sim$30 cm^{-1} (Jankowiak et al. 1993). SMS on PSI from *T. elongatus* at cryogenic temperature showed sharp emission lines and a broad unstructured intensity distribution. This broad intensity with typically more than 10 nm red-shift relative to the ZPLs cannot be identified with the PWs of the ZPLs. The sharp ZPLs in the range below 717 nm can be assigned to emitters absorbing around 708 nm (C708), whereas the broad intensity distributions can be assigned to more red-shifted emitters around 719 nm (C719) (Jelezko et al. 2000). The emitters of C708 are subject to spectral diffusion that changes their emission frequency with rates such that the spectral diffusion process can directly be monitored on single PSI complexes. The emitters of C719 undergo a spectral diffusion process that yields a severe broadening of the ZPLs within the acquisition time of a single spectrum and therefore only unresolved intensity distributions are observable. This difference points toward structural differences in the binding pockets of the chromophores responsible for C708 and C719 (Brecht et al. 2007).

In this contribution, we show ensemble as well as single molecule spectra of PSI from *Synechoccocus* sp. PCC 7002. The SM-spectra allow the distinction between two contributions to the fluorescence emission. These two pools show different sensitivity to the spectral diffusion process. Their properties resemble those observed recently for *T. elongatus*. Therefore, a structural analogy between the red pigments in *Synechoccocus* sp. PCC 7002 and in *T. elongatus* can be proposed.

Material and methods

PSI from the *Synechoccocus* sp. PCC 7002 has been isolated as described in Shen et al. 2002. Purified PSI trimers were at first diluted in buffer at pH 7.5 containing 20 mM Tricine, 25 mM $MgCl_2$, and 0.4 mM (0.02 % w/v) detergent (β-DM, Sigma), to reach a concentration of about 20 µM Chla. This amount of detergent is adequate for the critical solubilization concentration for a PSI trimer concentration of 0.5 µM, avoiding PSI aggregation (Muh and Zouni 2005). For pre-reduction of P700 5 mM Na-ascorbate was added. In further steps, this PSI containing solution was diluted to a PSI trimer concentration of 3 pM. Less than 1 µl of this sample was placed between two cover slips, assuring spatial separation of individual PSI trimers. Sample preparation and mounting were accomplished under indirect daylight. The experimental setup and the experimental conditions were recently described in Brecht et al. 2007. Absorption spectra at low temperature were recorded with a spectral resolution of 1 nm in a Cary-1E-UV/VIS spectrophotometer as described. Fluorescence spectra were recorded in a Fluoro-Max-2 (Jobin-Yvon). The sample was placed in a variable temperature liquid nitrogen bath cryostat (Oxford DN1704).

Results

Absorption and fluorescence emission spectra of PS I from *Synechoccocus* sp. PCC 7002 at 77 K are shown in Fig. 1. The absorption spectrum covers the region between 600 and 750 nm. The spectrum shows a strong peak in the region of the Q_y absorption-band of Chla at 680 nm.

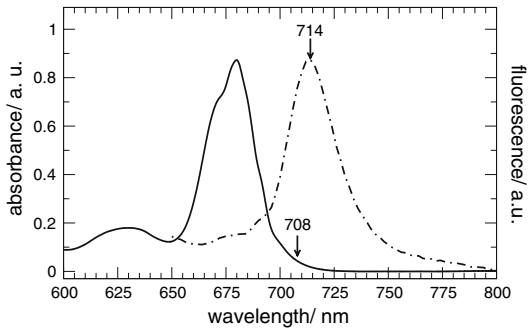

Fig. 1 77 K absorption spectrum (– line) and 77 K fluorescence emission spectrum (– · – line) of PS I from *Synechoccocus* sp. PCC 7002. The excitation was at 450 nm

Additional shoulders can be seen on the blue side (at 672 nm) and on the red side (at 692 nm) of the maximum. Above 700 nm the spectum exhibits a featureless red tail extending up to 720 nm. A decomposition of the absorption into gaussian bands shows that the intensity above 700 nm can be modeled by a single band with its maximum at 708 ± 4 nm (data not shown). Therefore this band is abbreviated by C708. About 2–3 Chla molecules contribute to the integrated absorption of C708. The fluorescence spectrum given in the range between 655–800 nm shows a broad band with Stokes-shifted maximum at 714 nm.

Single PSI complexes can be detected at low temperatures using the fluorescence emission of the red Chla (Jelezko et al. 2000). At low temperatures, these Chla molecules act as traps for the excitation energy and have a significant fluorescence quantum yield (Byrdin et al. 2000). Figure 2 shows a selection of five fluorescence emission spectra (denoted I–V) of single PSI complexes. The acquisition time for the spectra from the single complexes was between 20 and 30 s. For better comparability, the spectra were scaled to a similar magnitude. Each spectrum exhibits unique features, which will be described briefly. Spectrum I consists of a broad emission beginning with two steps at 690 nm and at 701 nm. Each of the steps shows a broadened ZPL at the high energy edge (at 692 nm and 702 nm). The maximum of the broad contribution is found at around 712 nm. Towards lower energy, a smooth decay of the fluorescence intensity is observed. Spectrum II consist of a broad intensity characterized by a steep increase between 690 and 697 nm. A ZPL with low intensity is found within the steep slope (at 697 nm). The broad emission shows two local maxima at 701 nm and 708 nm as well as a long tail into the red region. Spectrum III consists of a broad intensity distribution with an additional ZPL at 710 nm. A smooth intensity decrease is again observed at lower energies. Spectrum IV shows an intense ZPL at 693 nm followed by a slight increase of intensity that passes into a steep increase beginning at 701 nm and

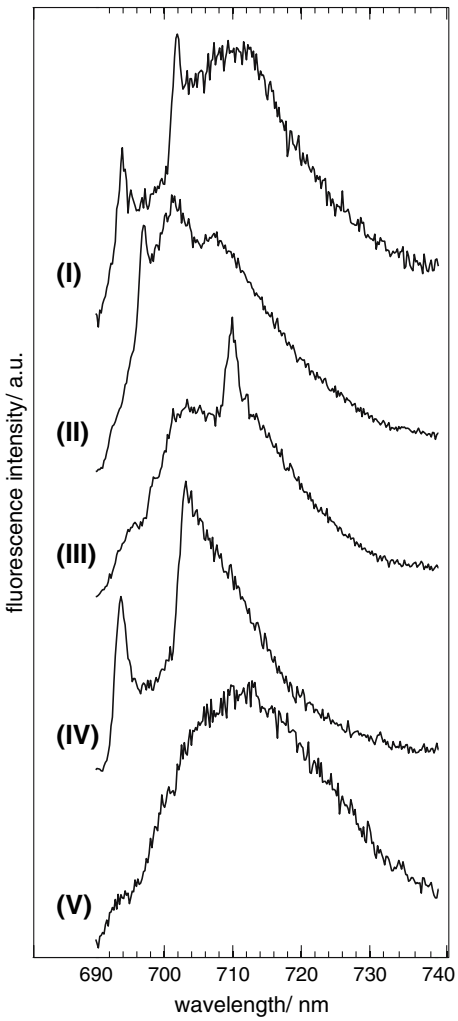

Fig. 2 Single-molecule fluorescence emission spectra of PS I complexes from *Synechoccocus* sp. PCC 7002. Spectra were recorded on different individual complexes at 1.4 K. Excitation was at 680 nm, and the accumulation time was between 20 and 30 s for each complex

ending at the maximum intensity of the spectrum at 703 nm. From there, an almost linear decrease of intensity is observed towards 720 nm. Spectrum V consists just of a single broad intensity distribution with its maximum at 712 nm.

The majority of fluorescence emission spectra recorded for single PSI complexes of *Synechoccocus* sp. PCC 7002 show resolved ZPLs on top of the broad main emission. In some spectra, ZPLs show up as intense narrow lines and in some spectra they are observed as broadened structures. The number of the ZPLs, their spectral position and line width varies from complex to complex. In spectra taken within 20–30 s the line width ranges from $\sim$ 0.2 nm up to some nanometers.

By reducing the accumulation time, the process of spectral diffusion can be suppressed in many cases. For the observation of spectral dynamics of individual ZPLs, it is useful to record time-dependent spectra (td spectra) in

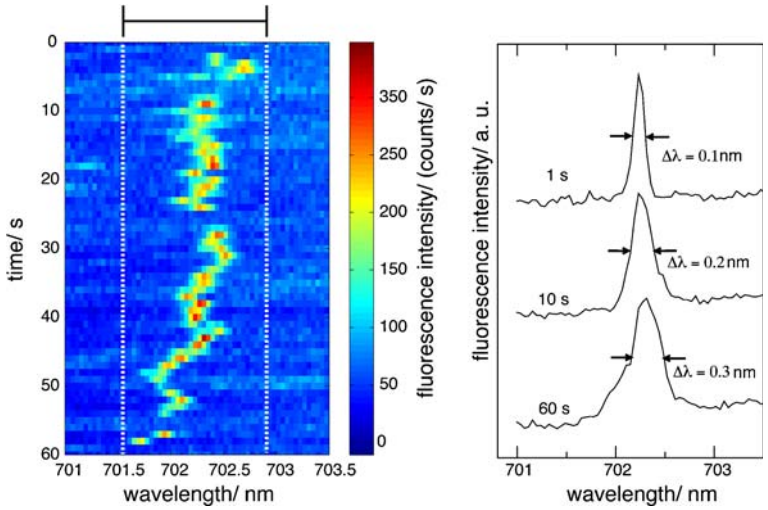

Fig. 3 Left: Plot of time-dependent fluorescence emission spectra of a PS I complex. The time sequence of 60 spectra with an accumulation time of 1 s for each spectrum is displayed. The vertical bar on top of the trail indicates the areas given by bars in Fig. 4A (see also text). Right: Spectra illustrating the line broadening by spectral diffusion. The spectrum on top is taken directly from the td spectra given on the left at the time position 40 s, so the accumulation time for this spectrum was 1 s. The spectrum in the middle is the result of the summation of the spectra in the time range 31–41 s and the spectrum at the bottom is the result of the summation of the whole data set (1–60 s). The excitation wavelength was 680 nm, T = 1.4 K

order to follow the spectral trails of the ZPLs. This was achieved by recording sequences of spectra with a time resolution of 1 s. The major fraction of td spectra taken for single PSI complexes shows time dependent movement of ZPLs. One of these td spectra is given in Fig. 3, showing representative examples of the dynamic behavior of ZPLs. The intensity of the ZPLs undergo remarkable variation during time. In some spectra, the line is missing completely (e.g., t = 25–26 s). In addition to the intensity variations, the wavelength position of the ZPL also varies with time. These variations show discrete wavelength jumps of the line (e.g., t = 57s and t = 58 s) as well as a Brownian motion-like shivering around a mean position (e.g., between 10 and 23 s). These processes modify the emission frequency of the ZPL and thus increase the line width in spectra taken with longer accumulation times. The process of line broadening is exemplified in the three spectra given on the right of Fig. 3. The spectrum on top is one single spectrum taken directly from the td spectrum on the left (at time t = 40 s). The ZPL in this spectrum has a line width of 0.1 nm. The spectrum in the middle is the result of the summation of the spectra in the interval 31–41 s. In this sum spectrum the line width has increased to 0.2 nm. The spectrum at the bottom results from the summation of all spectra given on the right (0–60 s). The line width has now increased to $\geq$ 0.3 nm.

The dynamic behavior of the ZPLs is very heterogeneous for single complexes. But, in general, we observe that the ZPLs remain in restricted spectral areas. In order to illustrate such a restricted area, white dashed lines have been included in the td spectrum as shown in Fig. 3. The range of the observed spectral trail of this ZPL spans from 701.6 to 702.9 nm, as indicated by the bar on top of the td spectrum. These type of ranges were determined from all recorded td spectra. The result of this analysis is shown in Fig. 4A. The determined ranges are given for each complex by bars. The spectral ranges occupied by the spectral trails of the ZPLs are in some cases well separated and in others they overlap. If the spectral trails are well separated, the bars represent the dynamic region of one single line. In the case of overlapping ranges, the ranges were combined and are given as one joint bar. Then a direct correlation of the width of a bar with the spectral band covered by an individual line is not possible. As can be seen in Fig. 4A, the extension and number of the spectral ranges covered by ZPLs vary from complex to complex.

The number of molecules showing a ZPL at a specific wavelength was determined (see figure caption) from Fig. 4A. The result is given in Fig. 4B. The obtained curve shows a clear spectral band that is formed by the ZPLs. The shape of this band can be fitted by a gaussian (dashed line) with maximum at 698 nm and the width of 4 nm. Therefore, the band is named F698. In the range $>$ 710 nm, the emission is dominated by broad intensity distributions. A ZPL was found in only four cases out of 36 analyzed td spectra (Fig. 4A).

An approach to quantify the number of emitters contributing to the fluorescence is a polarization analysis of the emission. Figure 5 shows the fluorescence emission from a single PSI complex and its dependence on the polarization.

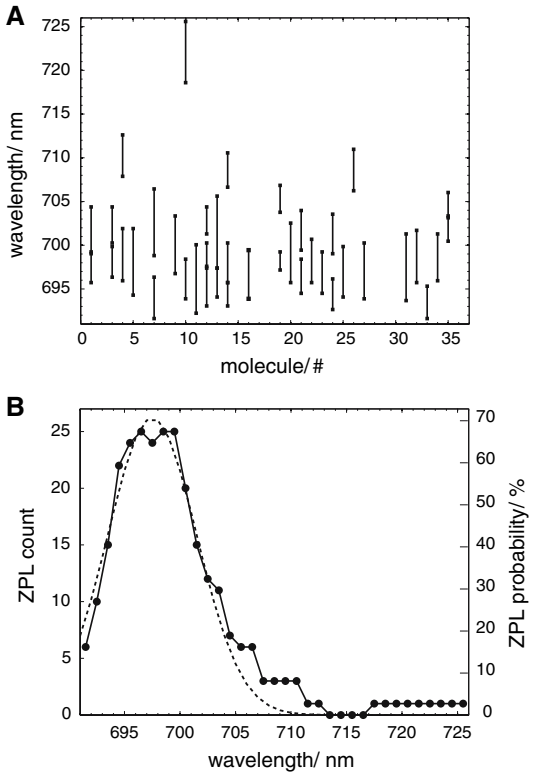

Fig. 4 (**A**) Statistical analysis of the distribution of ZPLs. The bars shows the individual regions in which ZPLs were observed in the td spectra of 36 individual PSI complexes. The determination of these areas from the td spectra is explained in the text and visualized in Fig. 3. (**B**) Number of molecules showing a ZPL at the given wavelength. The dots represent the number of bars shown in 4A at each wavelength using a bin size of 1 nm

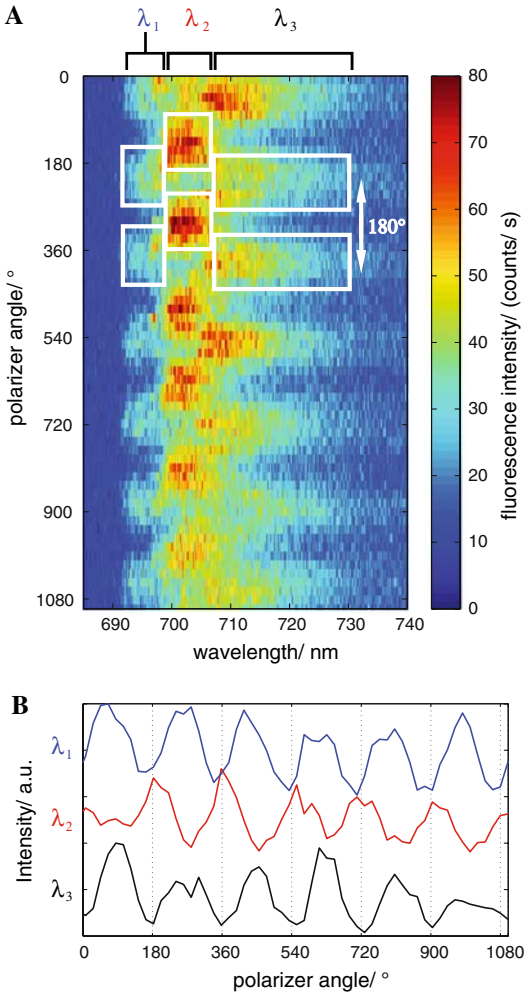

Fig. 5 (**A**) Sequence of fluorescence emission spectra of a single PSI complex from *Synechoccocus* sp. PCC 7002 as a function of the orientation of the polarizer in front of the spectrograph. The fluorescence intensity is encoded in the color scale on the right. The white squares included highlight the different spectral contributions during the first turn of the polarizer. (**B**) Integrated fluorescence intensity of the emission of a single PSI complex in the intervals indicated as λ_1, λ_2, and λ_3 as a function of the polarizer angle. The acquisition time for a single spectrum was 1 s

The polarizer angle given is defined with respect to an arbitrary laboratory axis and is uncorrelated to the polarization of the excitation light due to the preceding energy transfer steps. In Fig. 5A, the dependence of the whole emission as a function of the polarizer orientation is shown. Three contributions can be distinguished, they are highlighted by white squares in the picture for the first 360°. The observed emission is strongly polarized (Note: The fluorescence emission spectrum of the complex chosen for these polarization-dependent spectra was of the type V from Fig. 2, i.e., showed no resolved ZPLs). For this dataset, the integrated fluorescence intensity was determined for the ranges 691–699 nm (λ_1), 699–705 nm (λ_2), and 705–720 nm (λ_3), and is plotted in Fig. 5B. In this representation a sinusoidal shape of all curves can be seen; their periodicity is 180°. Similar strong polarization was observed for all PSI complexes investigated in this way. The emission found within the range λ_1 can be assigned to an emitter of F698, the emission within λ_2 can be either assigned to a member of F698 or to a member of C708. The emission within λ_3 is most probable due to an emitting state of C708. Due to the large inhomogeneous broadening of the observed pools, an assignment of emitters of one single complex always remains tentative. A strong polarization of the emitted light requires either a single emitter as origin of the emission, or a number of emitters with parallel transition dipole moments. Since the PSI complexes in our samples are randomly oriented, it is unlikely that the transition moments of several emitters would appear parallel in all cases.

Discussion

The 77 K absorption spectrum in Fig. 1 shows a high similarity with the absorption spectra from PSI complexes

from other cyanobacteria (e.g., Gobets and van Grondelle 2001). Interestingly, the most striking similarity is found between *Synechoccocus* sp. PCC 7002 and the PSI core of maize (Gobets and van Grondelle 2001). The absorption spectrum shows the contribution of 2–3 Chla species absorbing at lower energy than P700. The mean absorption of this pool is found at 708 ± 4 nm. The wavelength position of C708 is close to an observed pool position in *Synechocystis* sp. PCC 6803 (C706) (Hsin et al. 2004) and *T. elongatus* (C708) (Palsson et al. 1998). However, additional pools were found in PSI from *Synechocystis* sp. PCC 6803 as well as from *T. elongatus*. Such additional pools are lacking in *Synechoccocus* sp. PCC 7002. The total number of red Chla species per monomer is therefore higher for *T. elongatus* (7–9 per monomer) and *Synechocystis* sp. PCC 6803 (∼4) (Ratsep et al. 2000) than for *Synechoccocus* sp. PCC 7002.

The bulk fluorescence spectrum of *Synechoccocus* sp. PCC 7002 consists of an unstructured band with maximum at 714 nm. The maximum of the fluorescence emission of *Synechoccocus* sp. PCC 7002 is remarkably blue-shifted compared to the maximum position determined for PSI from *T. elongatus* and *Synechocystis* sp. PCC 6803, where the maxima were found at ∼730 nm (Zazubovich et al. 2002) and ∼718.5 nm (Gobets et al. 1994), respectively. Besides the large difference in the wavelength position, the shape of the fluorescence emission shows similarities between these different PSI complexes. The shift between the absorption C708 (*Synechoccocus* sp. PCC 7002) and the maximum of the fluorescence emission at 714 nm is about 6 nm, that is much larger than expected for monomeric Chla. The value found for *Synechoccocus* sp. PCC 7002 is between the shifts found for *T. elongatus*, where the maximum fluorescence emission and the absorption C719 are 11 nm apart and the 4.5 nm for C714 in *Synechocystis* sp. PCC 6803 (Zazubovich et al. 2002; Hayes et al. 2000).

The inhomogeneous broadening of the ensemble spectra can be lifted by SMS and the emission of single PSI complexes can be observed (Fig. 2). Most of the SM-spectra show a broad unresolved intensity distribution with broadened ZPLs superimposed on its blue side. The line width, spectral position and the intensity of the observed ZPLs vary from complex to complex. Spectral diffusion is the main broadening process for those ZPLs (Fig. 3). Recording of td spectra for single complexes (Fig. 3) shows, that the spectral diffusion process originates from spectral jumps of the ZPLs. The width of those jumps reach into the nm-range. For most of the ZPLs found in the region below 712 nm, the rate of this jump processes is in the range of our experimental time resolution (1 s). Such frequency jumps can be interpreted as hopping between different conformational substates of the protein (Frauenfelder et al. 1991; Hofmann et al. 2003). The spectral ranges that are accessible for the emitters in one complex due to hopping between the different substates can be extracted from the td spectra (Fig. 3). The shape of the energy landscape formed by the different conformational substates is highly individual for each complex, but general limitations for the hopping process of the ZPLs exist. The collection of all these confined areas (Fig. 4) form a spectral band. This spectral band has its center at 698 nm (F698). The spectral range covered by F698 represents only a small portion of the overall fluorescence emission of PSI from *Synechoccocus* sp. PCC 7002. The F698 Chla's probably belong to the pool giving rise to the shoulder at 692 nm in the 77 K absorption spectrum.

The spectral properties of F698 visible on the single molecule level show similarities with the emission of C708 from *T. elongatus*. The emission of both pools give rise to well resolved ZPLs in the spectra. In both cases these ZPLs reside on the blue wing of a broad emission. Comparing the time-dependent effects due spectral diffusion for the ZPLs from F698 and C708 (*T. elongatus*) shows that the rate as well as the width of the jumps are within the same range. Therefore, it can be assumed, that the chromophores of both pools show structural equivalence.

The dominant portion of the fluorescence intensity is emitted in broad intensity distributions. Such broad distributions are observed in almost all spectra (Fig. 2). The emission stems from the red-most state C708. Fluorescence emission spectra taken with a rotating polarizer in the front of the spectrograph show that the number of emitters responsible for the broad intensity distribution is small (Fig. 5). In the majority of cases, no indications for ZPLs were observed at wavelengths longer than 710 nm. The shape of F698 suggests that even those ZPLs observed in the region above 708 nm are due to emission from F698. In principle, each single emitter should give rise to a ZPL and a PW. However no ZPLs are observed for the broad intensity distributions. A similar behavior was observed by SMS for the emission of C719 in PSI complexes from *T. elongatus* (Brecht et al. 2007). Therefore, it was argued that a large electron-phonon coupling in conjunction with fast spectral diffusion could explain the absence of ZPLs in the spectra. For this explanation, line hopping of the corresponding ZPL must be much faster than the experimental time resolution, and the spectral ranges covered by these fast diffusing ZPLs must be close to the width of the corresponding broad intensity distribution (Brecht et al. 2007). These properties found for C719 resemble those observed for C708 (*Synechoccocus* sp. PCC 7002). Therefore, the structural composition of the chomophores of C708 in *Synechoccocus* sp. PCC 7002 must show an equivalence to

the chromophores associated with C719 in *T. elongatus*. Furthermore, this equivalence includes also the red-most pool C714 of *Synechocystis* sp. PCC 6803, because a structural similarity between C714 (*Synechocystis* sp. PCC 6803) and C719 (*T. elongatus*) was proposed based on hole-burning experiments (Zazubovich et al. 2002). In summary, it can be suggested that the red-most Chla in these three different PSI complexes possess a high structural equivalence, and this equivalence of the red-most pools is independent from the difference in red-shifts of these pools.

The observed properties can be interpreted within the picture of an energy landscape as follows: fast spectral diffusion occurs if the barrier between the conformational substates in the energy landscape are crossed with high rate and slow spectral diffusion occurs if the rate is low. The observed spectral width of one emitter corresponds to variations in the site-energy induced by conformation dynamics. In cases where the spectral width of a single emitter is close to the value observed in ensemble experiments, the energy landscapes have low barriers within a wide range of configurations. In cases where the spectral width is remarkably below the width of the ensemble experiments, the energy landscapes have some high barriers that cannot be crossed leading to confined intervals of emission wavelength. The chromophores of C708 show fast spectral diffusion and a large spectral width. This indicates a binding situation of the chromophores that results in higher flexibility than those with lower rates and restricted width. Recently, the emission of C719 was assigned to the strongly coupled dimers A38–A39 and B37–B38, which show a structural arrangement that allows high flexibility compared to that of other candidates for the long-wavelength chlorophylls (Brecht et al. 2007). Therefore, an assignment of C708 to these dimers is most reasonable. It should be noted that the two dimers A38–A39 and B37–B38 with most oscillator strength in the upper exciton band (Karapetyan et al. 2007) can explain only part of the intensity of the red-most band of the absorption spectra. The single emitters of F698 in *Synechoccocus* sp. PCC 7002 show slower spectral diffusion as well as smaller spectral width compared to C708. Therefore, the chomophores of this pool reside in a structural arrangement that is more rigid and are likely equivalent to those forming the C708 pool in *T. elongatus* as discussed above.

Acknowledgments We thank John H. Golbeck (Pennsylvania State University) for the PSI samples and helpful discussion and a reviewer for carefully reading the manuscript. This work was supported by Volkswagenstiftung in the framework of the program: Physics, chemistry, and biology with single molecules (I/78361 to R.B.) and by the Deutsche Forschungsgemeinschaft (SFB 498, TP A6 to E.S.).

References

Amunts A, Drory O, Nelson N (2007) The structure of a plant photosystem I supercomplex at 3.4 angstrom resolution. Nature 447(7140):58–63

Andrizhiyevskaya EG, Schwabe TME, Germano M, D'Haene S, Kruip J, van Grondelle R, Dekker JP (2002) Spectroscopic properties of PSI-IsiA supercomplexes from the cyanobacterium synechococcus pcc 7942. Biochim Biophys Acta Bioenerg 1556(2–3):265–272

Brecht M, Studier H, Elli AF, Jelezko F, Bittl R (2007) Assignment of red antenna states in photosystem I from thermosynechoccocus elongatus by single-molecule spectroscopy. Biochemistry 46(3):799–806

Brettel K (1997) Electron transfer and arrangement of the redox cofactors in photosystem I. Biochim Biophys Acta Bioenerg 1318(3):322–373

Byrdin M, Rimke I, Schlodder E, Stehlik D, Roelofs TA (2000) Decay kinetics and quantum yields of fluorescence in photosystem I from synechococcus elongatus with P700 in the reduced and oxidized state: Are the kinetics of excited state decay trap-limited or transfer-limited? Biophys J 79(2):992–1007

Frauenfelder H, Sliar SG, Wolynes PG (1991) The energy landscapes and motions of proteins. Science 254(5038):1598–1603

Fromme P, Jordan P, Krauss N (2001) Structure of photosystem I. Biochim Biophys Acta Bioenerg 1507(1–3):5–31

Gobets B, van Grondelle R (2001) Energy transfer and trapping in photosystem I. Biochim Biophys Acta Bioenerg 1507(1-3): 80–99

Gobets B, van Amerongen H, Monshouwer R, Kruip J, Rongner M, van Grondelle R, Dekker JP (1994) Polarized site-selected fluorescence spectroscopy of isolated photosystem-I particles. Biochim Biophys Acta Bioenerg 1188(1–2):75–85

Gobets B, van Stokkum IHM, van Mourik F, Dekker JP, van Grondelle R (2003) Excitation wavelength dependence of the fluorescence kinetics in photosystem I particles from synechocystis pcc 6803 and synechococcus elongatus. Biophys J 85(6): 3883–3898

Hayes JM, Matsuzaki S, Ratsep M, Small GJ (2000) Red chlorophyll a antenna states of photosystem I of the cyanobacterium synechocystis sp pcc 6803. J Phys Chem B 104(23):5625–5633

Hofmann C, Aartsma TJ, Michel H, Kohler J (2003) Direct observation of tiers in the energy landscape of a chromoprotein: A single-molecule study. Proc Natl Acad Sci USA 100(26): 15534–15538

Hsin TM, Zazubovich V, Hayes JM, Small GJ (2004) Red antenna states of PSI of cyanobacteria: Stark effect and interstate energy transfer. J Phys Chem B 108(29):10515–10521

Jankowiak R, Hayes JM, Small GJ (1993) Spectral hole-burning spectroscopy in amorphous molecular-solids and proteins. Chem Rev 93(4):1471–1502

Jelezko F, Tietz C, Gerken U, Wrachtrup J, Bittl R (2000) Single-molecule spectroscopy on photosystem I pigment-protein complexes. J Phys Chem B 104(34):8093–8096

Jordan P, Fromme P, Witt HT, Klukas O, Saenger W, Krauss N (2001) Three-dimensional structure of cyanobacterial photosystem I at 2.5 angstrom resolution. Nature 411(6840):909–917

Karapetyan NV, Schlodder E, van Grondelle R, Dekker JH (2007) Advances in photosynthesis and respiration vol 24, Photosystem I: the light-driven plastocyanin:ferredoxin oxidoreductase. Springer

Krauss N, Schubert WD, Klukas O, Fromme P, Witt HT, Saenger W (1996) Photosystem I at 4 angstrom resolution represents the first structural model of a joint photosynthetic reaction centre and core antenna, system. Nat Struct Biol 3(11):965–973

Melkozernov AN, Lin S, Blankenship RE (2000) Femtosecond transient spectroscopy and excitonic interactions in photosystem I. J Phys Chem B 104(7):1651–1656

Muh F, Zouni A (2005) Extinction coefficients and critical solubilisation concentrations of photosystems I and II from thermosynechococcus elongatus. Biochim Biophys Acta Bioenerg 1708(2):219–228

Palsson LO, Flemming C, Gobets B, van Grondelle R, Dekker JP, Schlodder E (1998) Energy transfer and charge separation in photosystem I: P700 oxidation upon selective excitation of the long-wavelength antenna chlorophylls of synechococcus elongatus. Biophys J 74(5):2611–2622

Ratsep M, Johnson TW, Chitnis PR, Small GJ (2000) The red-absorbing chlorophyll a antenna states of photosystem I: A hole-burning study of synechocystis sp pcc 6803 and its mutants. J Phys Chem B 104(4):836–847

Schlodder E, Shubin VV, El-Mohsnwy E, Roegner M, Karapetyan NV (2007) Steady-state and transient polarized absorption spectroscopy of photosystem I complexes from the cyanobacteria arthrospira platensis and thermosynechococcus elongatus. Biochim Biophys Acta 1767(6):732–741

Sener MK, Lu DY, Ritz T, Park S, Fromme P, Schulten K (2002) Robustness and optimality of light harvesting in cyanobacterial photosystem I. J Phys Chem B 106(32):7948–7960

Shen GZ, Zhao JD, Reimer SK, Antonkine ML, Cai Q, Weiland SM, Golbeck JH, Bryant DA (2002) Assembly of photosystem I: II. inactivation of the ruba gene encoding a membrane-associated rubredoxin in the cyanobacterium synechococcus sp pcc 7002 causes a loss of photosystem I activity. J Biol Chem 277(23):20343–20354

Tamarat P, Maali A, Lounis B, Orrit M (2000) Ten years of single-molecule spectroscopy. J Phys Chem A 104(1):1–16

Zazubovich V, Matsuzaki S, Johnson TW, Hayes JM, Chitnis PR, Small GJ (2002) Red antenna states of photosystem I from cyanobacterium synechococcus elongatus: a spectral hole burning study. Chem Phys 275(1–3):47–59